International Journal of Electrochemical Science 19 (2024) 100585

Contents lists available at ScienceDirect

International Journal of Electrochemical Science

journal homepage: www.editorialmanager.com/ijoes

Enhanced carbon monoxide tolerance of platinum nanoparticles synthesized through the Flash Joule Heating Method

Julio Nandenha [a], Gabriel Silvestrin [a], Larissa Otubo [a], Delvonei A. Andrade [a], Rodrigo F.B. de Souza [a], Ermete Antolini [b], Almir O. Neto [a,*]

[a] Instituto de Pesquisas Energerticas e Nucleares, IPEN/CNEN-SP, Av. Prof. Lineu Prestes, 2242 Cidade Universitaria, São Paulo, SP CEP 05508-900, Brazil
[b] ScuolaScienzaMateriali, Via 25 aprile 22, Genova, Cogoleto 16016, Italy

ARTICLE INFO

Keywords:
Pt electrocatalys
Flash Joule Heating Method
Carbon Monoxide
Fuel Cell
Cyclic Voltammetry

ABSTRACT

Was employ the Flash Joule Heating Method (FJHM) to synthesize carbon-supported Pt nanoparticles. In this method, an aqueous solution of the Pt precursor$H_2PtCl_6{\cdot}6\ H_2O$ is introduced into a reactor containing Vulcan XC 72 carbon. Subsequently, the mixture undergoes 50 cycles of discharges at 100 coulombs per discharge. Comparative XRD analysis with a commercially prepared Pt/C BASF, utilizing a reduction deposition method, reveals an expansion in the interplanar spacing of the platinum crystal lattice in the FJHM-prepared Pt/C catalyst (FJHM-Pt/C). This expansion suggests the emergence of structural defects, a finding confirmed by TEM images displaying distinct step-like features on the FJHM-Pt/C surface. Cyclic voltammogram analysis demonstrates a noteworthy increase in the oxidation pre-peak at 0.5 V for FJHM-Pt/C compared to Pt/C BASF. When employing pure H_2 as fuel, the single proton exchange membrane fuel cell (PEMFC) utilizing Pt/C BASF as the anode catalyst exhibits a higher maximum power density (MPD) than its FJHM-Pt/C counterpart. Conversely, in the presence of CO, the PEMFC with FJHM-Pt/C as the catalyst demonstrates a superior MPD compared to the cell equipped with commercial Pt/C as the anode. These findings underscore enhanced CO tolerance, highlighting the potential advantages of the FJHM preparation method.

1. Introduction

Polymer electrolyte membrane fuel cells (PEMFCs) are suitable device for energy conversion, thanks to their high-power density, efficiency, and operational viability even at low temperatures. However, the introduction should delve deeper into the needs and challenges surrounding these fuel cells. Notably, extensive research has been conducted on the development of electrocatalysts rich in defects, signifying a significant area of advancement in this field [1].

Platinum serves as a common catalyst at both the anode and cathode, facilitating the oxidation of hydrogen and the reduction of oxygen, respectively. However, the presence of impurities like carbon monoxide (CO), primarily derived from the catalytic reforming of hydrocarbons to obtain hydrogen, poses a challenge. CO adsorption on the platinum catalyst's active sites reduces the performance of the fuel cell at the anode [2].

In the 1990 s, studies on platinum single crystals [3–5] highlighted Pt (111) as the most active plane for CO oxidation, suggesting potential strategies for enhancing catalytic processes. However, the application of such strategies, such as introducing steps and terraces to favor CO oxidation at less positive potentials [6], proved impractical for nanoparticle synthesis. This underscores the need for alternative approaches to mitigate CO adsorption on platinum surfaces.

A strategy to mitigate the issue of CO adsorption on platinum nanoparticles surfaces involves the development of binary and ternary Pt-based catalysts, such as PtRu, PtMo, and PtRuMo [7–12]. The presence of a second/third metal modifies the CO adsorption characteristics of Pt nanoparticles, with this effect attributed to reaction with surface oxy-hydroxyl species formed at less positive potentials than pure platinum [13], and/or by modifying the d-band of the noble metal, altering its affinity for CO adsorption [14]. In addition to Pt, other metals such as Ir, Te, Cu, Fe, and Rh have been studied for this purpose [15–18].

A common method to prepare these electrocatalysts involves the utilization of sodium borohydride as a reducing agent for both Pt and the second/third metal precursors [19,20]. Other method involves the process of spontaneous deposition of the second metal by immersing the

* Corresponding author.
E-mail address: aolivei@usp.br (A.O. Neto).

https://doi.org/10.1016/j.ijoes.2024.100585
Received 6 February 2024; Received in revised form 11 April 2024; Accepted 11 April 2024
Available online 12 April 2024

platinum electrode within a solution that contains a ruthenium salt, leading to the irreversible adsorption of Ru onto the Pt surface [21]. In contrast, the forced deposition approach involves submerging the Pt electrode in an electrolyte under the presence of hydrogen bubbling or exposing the wet sample to a stream of H_2 gas [22]. This leads to the creation of a suitably reducing potential that promotes the direct deposition of Ru species onto the electrode. Both techniques predominantly employ Pt single-crystal surfaces as the preferred substrate [23]. Another approach entails the use of transition metal oxides, nitrides, carbides, or phosphides as co-catalysts. These co-catalysts serve to enhance the overall catalytic activity and selectivity of the Pt-based catalysts, particularly by influencing the adsorption properties of CO and other relevant species [24,25].

Ramos et al. [18] reported a novel approach involving the utilization of a sodium borohydride reducing agent in conjunction with a magnetic field and radiofrequency pulse. This study revealed a compression of lattice strain within the Pt crystallographic structure. As a result, the adsorption energy of CO on Pt/C was potentially attenuated. This outcome might be attributed to the introduction of structural defects, suggesting a correlation between lattice strain manipulation and CO adsorption behavior. Li et al. [26] showed that a Joule heating technique could induce the fragmentation of metal precursors, thereby facilitating the uniform blending of constituent elements. This is followed by a swift cooling phase, which facilitates the creation of precisely defined crystalline nanoparticles.

Qiu et al. [27] synthesized an Ag/Co/C electrocatalyst using the flash Joule heating method for the oxygen reduction reaction within an alkaline environment. Thishybrid catalyst delivereda specific activity that exceeded that of the pristine Ag/C by 40 times, and its mass activity surpassed the reference material by 52 times at 0.8 V vs. RHE in alkaline media. Additionally, the hybrid catalyst showed enhanced tolerance to methanol and ethanol compared to commercially available Pt/C electrocatalysts. In the present work, for the first time a Pt/C electrocatalyst was prepared using the Flash Joule Heating process in a device developed within our research group. Theaim is to synthesize a catalyst with defects, thereby enhancing the activity for the oxidation of the H_2+CO mixture originating from catalytic reforming.

2. Experimental

The Pt/C 20 % electrocatalyst was prepared using a Flash Joule Heating Method, a technique involving the placement of appropriate amounts of the metal precursor H2PtCl6.6H2O (Aldrich) and water in a 1:1 (w/w) ratio onto a quantity of Vulcan XC-72 carbon to obtain a catalyst with a 20 % loading in a graphite crucible. The crucible is then sealed and subjected to 50 discharge cycles at 100 coulombs per discharge at 65 V, for a total time of 60 seconds [28]. The charge-to-electron ratio required for the metal reduction is 2 per discharge. Subsequently, the obtained FJHM - Pt/C catalyst was subjected to characterization.

The platinum load on carbon was determinedby thermogravimetric analysis performed on a SETARAM LABSYS. The samples were heated from 25 to 900 °C at aconstant rate of 10 °C per minute. The electrocatalysts were characterized through X-ray diffraction (XRD) utilizing a Rigaku Miniflex II diffractometer equipped with a Cu Kα source (λ = 1.54056 Å) at a 2θ range spanning from 20° to 90°, employing a step size of 0.02° and a scan duration of 2 seconds per step. Transmission Electron Microscopy (TEM) analysis was carried out employing a JEOL electron microscope model JEM-2100.

Cyclic voltammetry measurements were carried out at a temperature of 25°C, employing an Autolab PGSTAT 302 potentiostat/galvanostat. The working electrode comprised a vitreous carbon (0.2 cm^2) material with a deposited porous ultrathin layer [29] in a aliquot of 20 μl. The reference electrode employed was the reversible hydrogen electrode (RHE), while the counter electrode took the form of a platinum (Pt) plate. These electrochemical analyses were performed within

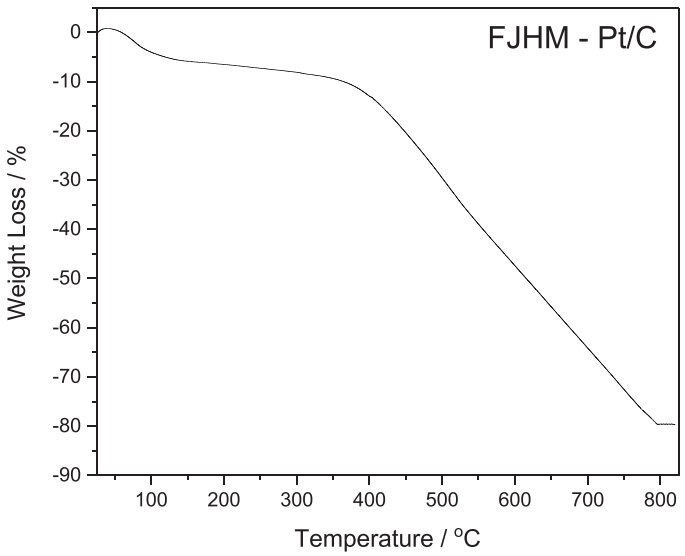

Fig. 1. Thermogravimetric analysis of FJHM-Pt/C.

0.5 mol L^{-1} H_2SO_4 solutions saturated with nitrogen (N_2). For CO-stripping experiments, the working electrode was purged with N_2 for 30 minutes, then exposed to purified CO gas for an additional 30 minutes, with the working electrode potential set at 0.2 V vs. RHE. Following the adsorption process, CO was purged from the electrolyte solution, subsequently submitted to 15 minutes of N_2 bubbling. The CO-stripping voltammograms were recorded using a scan rate of 10 mV s^{-1}.

The fuel cell experiments were performed utilizing Pt/C materials synthesized by Flash Joule Heating Method for the anode and commercial Pt/C (BASF) for the cathode. A hydrogen flux of 300 mL min^{-1} was employed for the anode, while the cathode utilized an oxygen flux of 200 mL min^{-1}. Tests were carried out in a single PEMFC, featuring electrodes with an active geometric surface area of 5.0 cm^2. The gas diffusion layer comprised PTFE-treated carbon cloth, and the electrolyte involved a Nafion® 117 membrane.

For the fuel cell investigations, both the anode and cathode utilized electrodes loaded with 1.0 mg_{Pt} cm^{-2} of electrocatalyst. In experiments involving the synthesis gas (H_2+CO), atmospheric pressure was

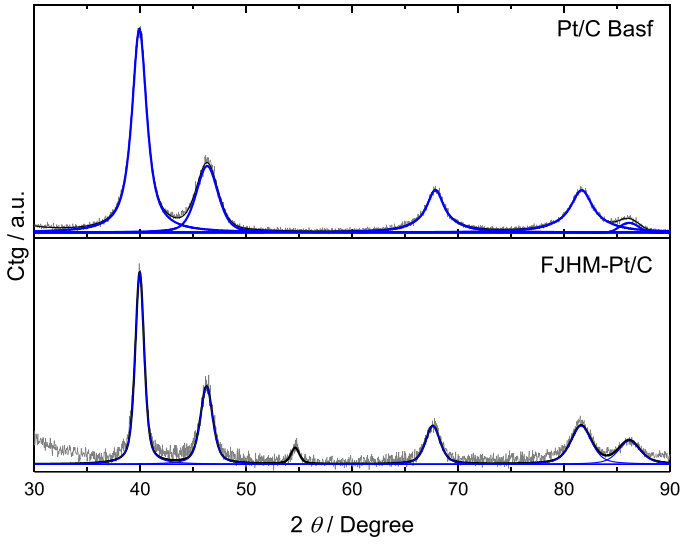

Fig. 2. X-ray diffractions pattern of Pt/C BASF and FJHM-Pt/C. In grey measured data, in black fited data, and in blue the function corresponding for each platinum peak.

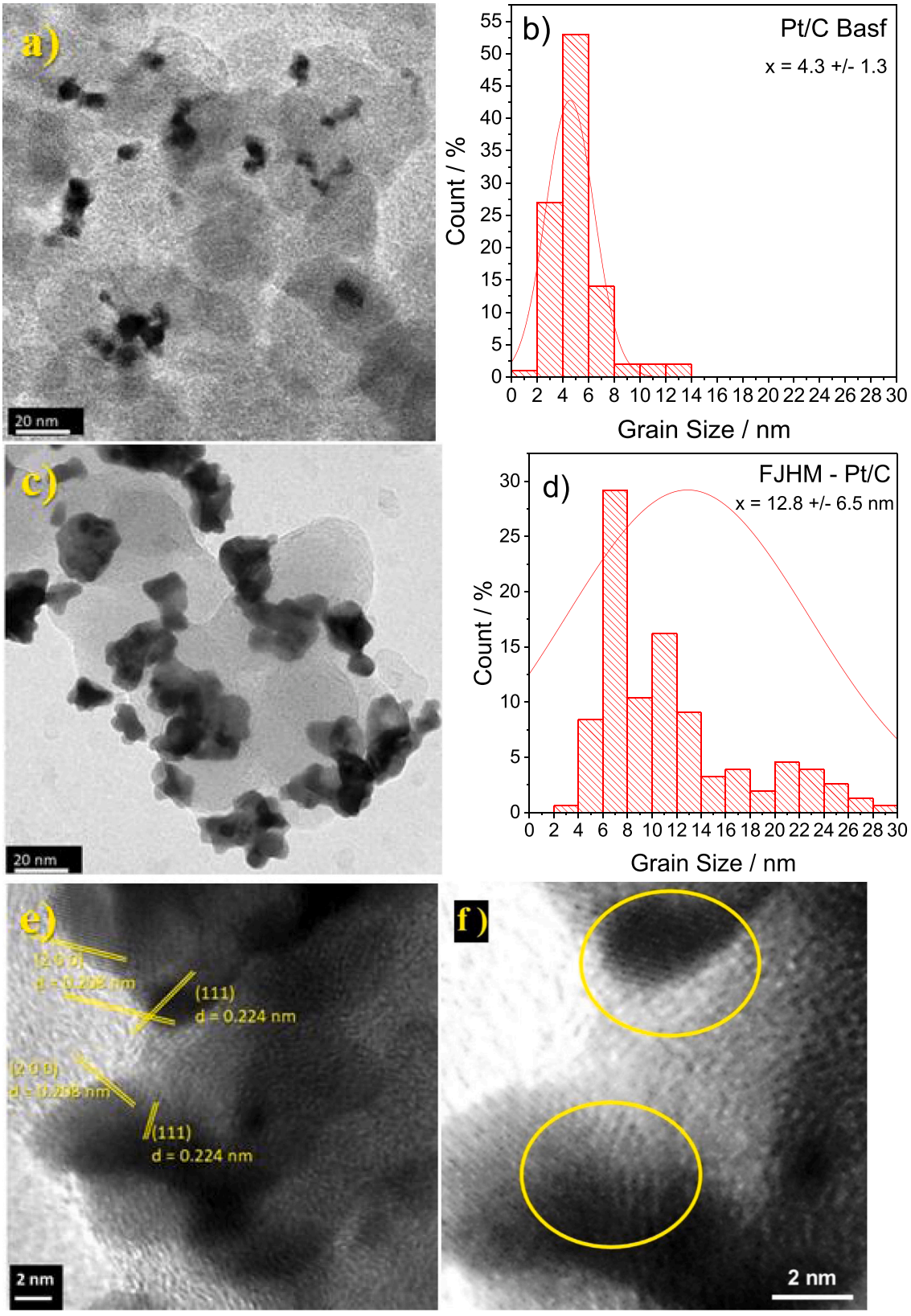

Fig. 3. a) TEM of Pt/C BASF, b) histogram of size distribution of Pt/C BASF, c) TEM of FJHM-Pt/C, b) histogram of size distribution of FJHM-Pt/C, e) TEM image of FJHM-Pt/C with d-space and plane highlighted, f) marking of interplanar crossings in the TEM image of FHJM-Pt/C.

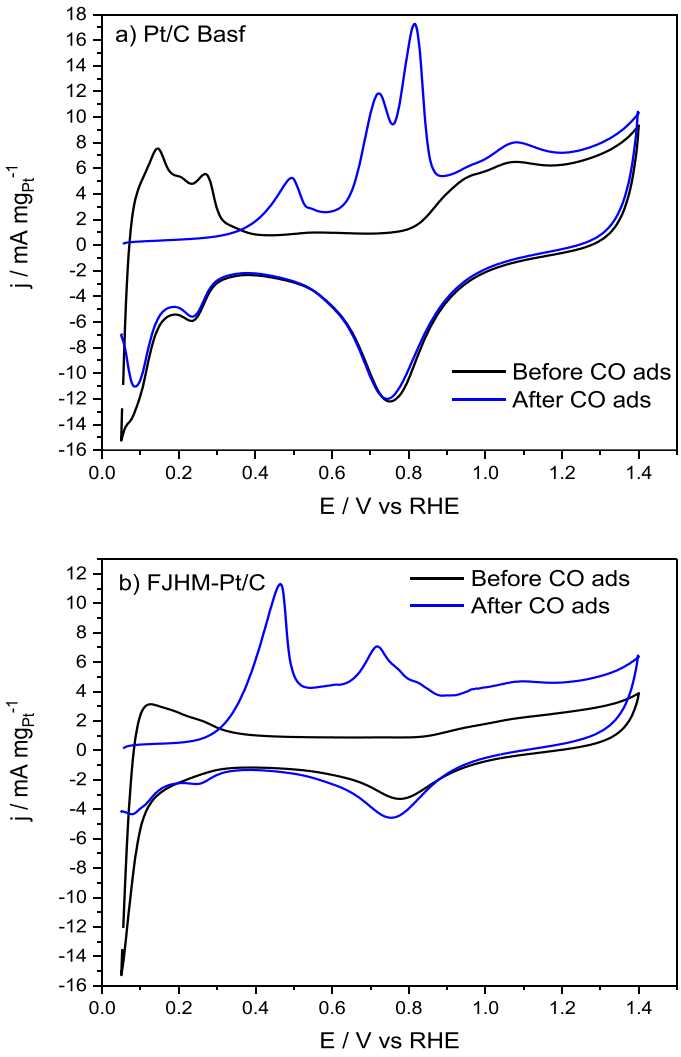

Fig. 4. Cyclic voltammetry of Pt/C BASF and FJHM-Pt/C in 0.5 mol L^{-1} H_2SO_4, v = 10 mV s^{-1}.

maintained at the anode and cathode. The operating temperature of the fuel cell was set at 80°C, with the flux of H_2+CO (with CO at 100 ppm) regulated at 300 mL min^{-1} for the anode, and O_2 flux set at 200 mL min^{-1} for the cathode. Pt/C was prepared in triplicate, and these distinct batches were characterized simultaneously with an error margin of less than 10 %.

3. Results and discussion

As a novel synthesis method, the FJHM-Pt/C material was submitted to a thermographic analysis to verify the metal-to-carbon ratio. The weight loss of the electrocatalyst (Fig. 1) initiates below 100°C as a result of the desorption of adsorbed water [30]. Noticeably, substantial mass reductions occur at approximately 230 °C due to the decomposition and evolution of CO and CO_2 from the carbon support. After the depletion of carbon, the mass remained constant at 79.5 %, indicating a platinum content of ~ 20 %, and that during the synthesis there is no loss of carbon or platinum.

The XRD patterns of FJHM-Pt/C and, for comparison, of a commercial Pt/C (BASF), prepared by a reduction-deposition method [30] are shown in Fig. 2. The diffraction patterns revealed distinct peaks at 2θ angles of approximately 40°, 47°, 67°, 82°, and 86°, corresponding to the (111), (200), (220), and (311) planes of a face-centered cubic (FCC) structure. The Pt/C BASF sample aligned with the reference parameters JCPDS #87–647, featuring d-spacing values of 0.230, 0.194, 0.138, 0.117, and 0.112 nm for the (111), (200), (220), (311), and (222) planes, respectively.

In contrast, FJHM-Pt/C exhibited noticeable shifts toward more negative values in the 2θ angles for the (200), (220), (311), and (222) planes, while the (111) plane displays a shift towards more positive angles when compared to Pt/C BASF. This shift strongly suggests alterations in the lattice parameters of the crystal structure, with FJHM-Pt/C featuring d-spacing values of 0.224, 0.208, 0.142, 0.125, and 0.115 nm. It is valid to add that in the diffractogram of the FJHM material, a peak appears at ~54° corresponding to the 101 plane of graphitized carbon.

An additional significant observation was the prominence of the (222) plane peak, which appears considerably larger than that observed for the commercial Pt/C. To elucidate this, the relative intensities of the (111), (200), (220), (311), and (222) planes was calculated. In the case of commercial Pt/C, these planes showed relative intensities of 100, 42, 30, 28, and 5 %, respectively, while for FJHM-Pt/C, the corresponding values were 100, 56, 32, 45, and 29 %. This discrepancy indicates that the particle production method employed here discourages the formation of the (111) plane while favoring the high-index planes such as (311) and (222). These changes in the lattice parameters and relative plane intensities strongly suggest that the Flash Joule Heating method induced structural modifications in the platinum nanoparticles. Such structural alterations may lead to the emergence of structural defects, a phenomenon well-documented in the literature, which has the potential to influence the catalytic properties of the material [31,32].

Fig. 3 displays transmission electron microscopy (TEM) images for both Pt/C BASF and FJHM-Pt/C. Both materials showed a well-dispersed distribution on the support. However, the particles in the FJHM-Pt/C catalyst were significantly larger in size and feature prominent corners, whereas the Pt/C BASF nanoparticles presented rounded shapes. The pronounced corners in the FJHM-Pt/C nanoparticles could be attributed to a rapid and forced reduction process induced by the electron cascade resulting from the discharges during synthesis.

Additionally, intriguingly, the TEM images of the FJHM-Pt/C catalyst revealed the presence of distinctive step-like features (Fig. 3f), which can be interpreted as indicative of defects within the crystal structure of the electrocatalyst. These findings prompt a more in-depth exploration of the impact of these structural differences on the electrocatalytic properties and performance of Pt/C in various applications.

Fig. 4 shows the cyclic voltammetry of Pt/C BASF and FJHM-Pt/C nanoparticles during CO adsorption and desorption in a 0.5 mol L^{-1} H_2SO_4 aqueous solution. In the absence of CO (depicted by the black line), a well-defined hydrogen adsorption and desorption region ranging from 0.05 to 0.4 V wasclearly observed [18,30]. In the case of the FJHM-Pt/C catalyst, a reduction in the sharpness of the hydrogen adsorption and desorption peaks can be observed. This modification can be attributed to changes in the relative abundance of crystallographic facets or to defects generated during the particle formation process.

In the case of the commercial Pt/C and its CO oxidation behavior, it is possible to observe the typical pre-peak centered at 0.5 V, along with two additional higher peaks at 0.75 V and 0.85 V. However, when examining FJHM-Pt/C, a notably strong peak emerges at 0.45 V, which is significantly larger than that observed for Pt/C. Additionally, there are two less intense peaks at approximately 0.72 V and 0.82 V, corresponding to those observed for commercial Pt/C. This heightened peak at 0.45 V in FJHM-Pt/C, when compared to Pt/C BASF, suggests that a substantial portion of the adsorbed intermediates has been oxidized at lower potential values. Cudero et al. [33,34] have shown that the pre-peak corresponds to the oxidation of adsorbed CO, primarily resulting from its reaction with oxygenated species that initially nucleate at step sites. The appearance of the main peak coincides with the nucleation of oxygenated species not only at step sites but also on the terrace regions[34]. The presence of the pre-peak may also indicate an increase in structural defects within the electrocatalyst.

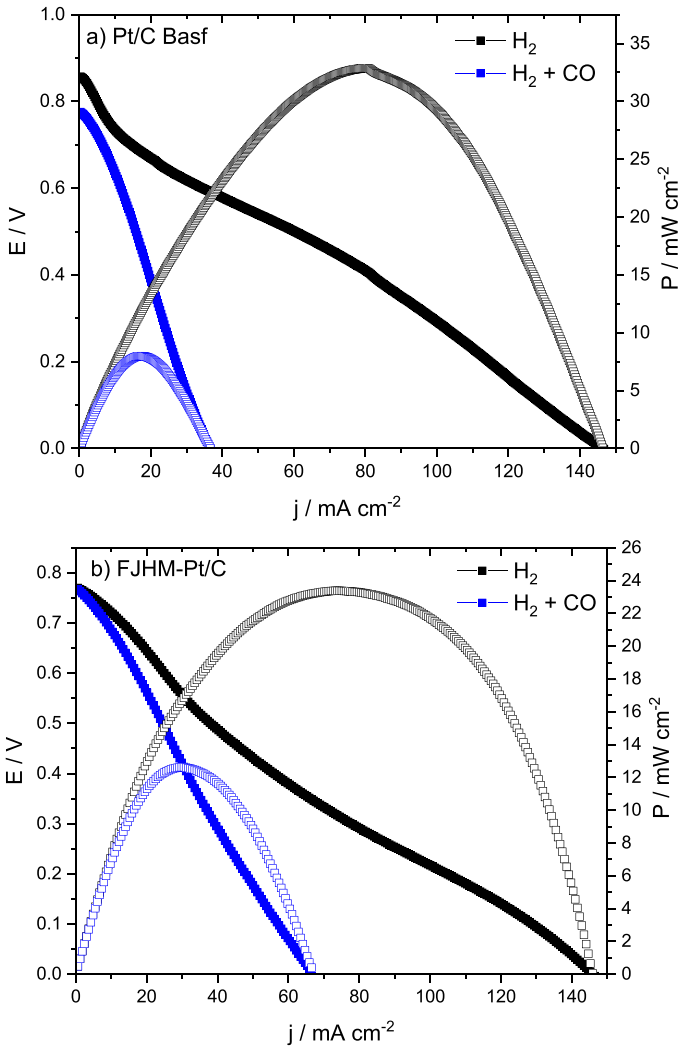

Fig. 5. Polarization and power density curves for PEMFCs with Pt/C BASF and FJHM-Pt/C as the anode catalyst. The black lines represent the H_2 experiment and the blue lines H_2+CO experiment.

Fig. 5 presents the polarization and power density curves for PEMFCs with both Pt/C BASF and FJHM-Pt/C as anode catalysts. In the case of pure H_2, the cell with the commercial Pt/C electrocatalyst showed a remarkable maximum power density (MPD) of approximately 32 mW cm^{-2} and an open-circuit potential of 0.85 V. Conversely, the cell with FJHM-Pt/C catalyst delivered a lower MPD of 22 mW cm^{-2}, about 31 % smaller than that of the cell with Pt/C BASF, and a reduced open-circuit potential to 0.75 V. These results emphasize the superior performance of the Pt BASF electrocatalyst for pure hydrogen oxidation, which can likely be attributed to its considerably smaller average particle size compared to FJHM-Pt/C.

However, when the oxidation of an H_2+CO mixture in a single PEMFC was evaluated, an opposite result was observed. The FJHM-Pt/C electrocatalyst delivered a higher MPD (13.0 mW cm^{-2}) compared to the commercial Pt/C electrocatalyst (8.0 mW cm^{-2}). The reduction in maximum power density for the Pt/C BASF was approximately 75 %, whereas for FJHM-Pt/C was 46 %. This suggests an improved tolerance to CO. This intriguing observation aligns with the cyclic voltammetry results. Several factors may contribute to this phenomenon, including the presence of surface defects, adlayers with varying crystallographic orientations, and/or strong metal/support interactions [18,35–38]. These factors likely play a role in a complex, multi-step CO oxidation process on the Pt catalyst surface.

4. Conclusion

The Flash Joule Heating Method enabled the preparation of an effective platinum electrocatalyst for the oxidation of the H_2+CO mixture. The thermographic analysis confirmed the metal load of 20 %. X-ray diffraction revealed significant shifts in the diffraction angles for specific crystallographic planes in FJHM-Pt/C compared to Pt/C BASF. Notably, the (222) plane exhibited a more prominent peak in FJHM-Pt/C, suggesting a preference for high-index planes.TEM images further demonstrated that the FJHM-Pt/C particles were larger and featured prominent corners, while the commercial Pt/C particles had rounded shapes. Regarding CO oxidation behavior, FJHM-Pt/C exhibited a stronger peak at 0.45 V, indicating a higher ability for CO oxidation compared to Pt/C BASF. In single PEMFC tests with pure H_2, the commercial Pt/C outperformed FJHM-Pt/C, likely due to its smaller average particle size. However, in the presence of CO, the cell with the FJHM-Pt/C catalyst displayed a higher power density, indicating an enhanced CO tolerance. This result can be attributed to various factors, including Pt structural defects and metal-support interactions.

Declaration of Competing Interest

The authors declare that they have no known competing financial interests or personal relationships that could have appeared to influence the work reported in this paper.

Acknowledgements

We are grateful to CAPES, CNPq (350514/2023-2, 302709/2020-7) for financial support of this work.

References

[1] Y. Wang, Y. Pang, H. Xu, A. Martinez, K.S. Chen, PEM Fuel cell and electrolysis cell technologies and hydrogen infrastructure development – a review, Energy Environ. Sci. 15 (2022) 2288–2328, https://doi.org/10.1039/D2EE00790H.
[2] A. Pei, L. Ruan, B. Liu, W. Chen, S. Lin, B. Chen, Y. Liu, L.H. Zhu, B.H. Chen, Ultra-low Au decorated PtNi alloy nanoparticles on carbon for high-efficiency electro-oxidation of methanol and formic acid, Int. J. Hydrog. Energy 45 (2020) 22893–22905, https://doi.org/10.1016/j.ijhydene.2020.06.164.
[3] H. Kita, H. Naohara, T. Nakato, S. Taguchi, A. Aramata, Effects of adsorbed CO on hydrogen ionization and CO oxidation reactions at Pt single-crystal electrodes in acidic solution, J. Electroanal. Chem. 386 (1995) 197–206, https://doi.org/10.1016/0022-0728(94)03813-I.
[4] S.-G. Sun, Y.-Y. Yang, Studies of kinetics of HCOOH oxidation on Pt(100), Pt(110), Pt(111), Pt(510) and Pt(911) single crystal electrodes, J. Electroanal. Chem. 467 (1999) 121–131, https://doi.org/10.1016/S0022-0728(99)00032-7.
[5] A.M. de Becdelièvre, J. de Becdelièvre, J. Clavilier, Electrochemical oxidation of adsorbed carbon monoxide on platinum spherical single crystals: effect of anion adsorption, J. Electroanal. Chem. Interfacial Electrochem. 294 (1990) 97–110, https://doi.org/10.1016/0022-0728(90)87138-A.
[6] N.P. Lebedeva, M.T.M. Koper, E. Herrero, J.M. Feliu, R.A. van Santen, Cooxidation on stepped Pt[n(111)×(111)] electrodes, J. Electroanal. Chem. 487 (2000) 37–44, https://doi.org/10.1016/S0022-0728(00)00149-2.
[7] J.-H. Wee, K.-Y. Lee, Overview of the development of CO-tolerant anode electrocatalysts for proton-exchange membrane fuel cells, J. Power Sources 157 (2006) 128–135, https://doi.org/10.1016/j.jpowsour.2005.08.010.
[8] T. Ioroi, T. Akita, S.-i Yamazaki, Z. Siroma, N. Fujiwara, K. Yasuda, Comparative study of carbon-supported Pt/Mo-oxide and PtRu for use as CO-tolerant anode catalysts, Electrochim. Acta 52 (2006) 491–498, https://doi.org/10.1016/j.electacta.2006.05.030.
[9] J.E. Hu, Z. Liu, B.W. Eichhorn, G.S. Jackson, CO tolerance of nano-architectured Pt–Mo anode electrocatalysts for PEM fuel cells, Int. J. Hydrog. Energy 37 (2012) 11268–11275, https://doi.org/10.1016/j.ijhydene.2012.04.094.
[10] N. Narischat, T. Takeguchi, T. Mori, S. Iwamura, I. Ogino, S.R. Mukai, W. Ueda, Effect of the mesopores of carbon supports on the CO tolerance of Pt2Ru3 polymer electrolyte fuel cell anode catalyst, Int. J. Hydrog. Energy 41 (2016) 13697–13704, https://doi.org/10.1016/j.ijhydene.2016.05.272.
[11] M. González-Hernández, E. Antolini, J. Perez, Synthesis, Characterization and CO Tolerance Evaluation in PEMFCs of Pt2RuMo Electrocatalysts, Catalysts (2019), https://doi.org/10.3390/catal9010061.
[12] M. González-Hernández, E. Antolini, J. Perez, CO tolerance and stability of PtRu and PtRuMo electrocatalysts supported on N-doped graphene nanoplatelets for polymer electrolyte membrane fuel cells, Int. J. Hydrog. Energy 45 (2020) 5276–5284, https://doi.org/10.1016/j.ijhydene.2019.05.208.

[13] L.G.S. Pereira, V.A. Paganin, E.A. Ticianelli, Investigation of the CO tolerance mechanism at several Pt-based bimetallic anode electrocatalysts in a PEM fuel cell, Electrochim. Acta 54 (2009) 1992–1998, https://doi.org/10.1016/j.electacta.2008.07.003.
[14] X. Zhang, H. Li, J. Yang, Y. Lei, C. Wang, J. Wang, Y. Tang, Z. Mao, Recent advances in Pt-based electrocatalysts for PEMFCs, RSC Adv. 11 (2021) 13316–13328, https://doi.org/10.1039/D0RA05468B.
[15] X. Yang, Y. Wang, X. Wang, B. Mei, E. Luo, Y. Li, Q. Meng, Z. Jin, Z. Jiang, C. Liu, J. Ge, W. Xing, CO-Tolerant PEMFC anodes enabled by synergistic catalysis between iridium single-atom sites and nanoparticles, Angew. Chem. Int. Ed. 60 (2021) 26177–26183, https://doi.org/10.1002/anie.202110900.
[16] S.M. Brkovic, M.P. Marceta Kaninski, P.Z. Lausevic, A.B. Saponjic, A.M. Radulovic, A.A. Rakic, I.A. Pasti, V.M Nikolic, Non-stoichiometric tungsten-carbide-oxide-supported Pt–Ru anode catalysts for PEM fuel cells – from basic electrochemistry to fuel cell performance, Int. J. Hydrog. Energy 45 (2020) 13929–13938, https://doi.org/10.1016/j.ijhydene.2020.03.086.
[17] P.J. Sarma, C.L. Gardner, S. Chugh, A. Sharma, E. Kjeang, Strategic implementation of pulsed oxidation for mitigation of CO poisoning in polymer electrolyte fuel cells, J. Power Sources 468 (2020) 228352, https://doi.org/10.1016/j.jpowsour.2020.228352.
[18] A.S. Ramos, M.C.L. Santos, C.M. Godoi, L.C. de Queiroz, J. Nandenha, E.H. Fontes, W.R. Brito, M.B. Machado, A.O. Neto, R.F.B. de Souza, High CO tolerance of Pt nanoparticles synthesized by sodium borohydride in a time-domain NMR spectrometer, Int. J. Hydrog. Energy 45 (2020) 22973–22978, https://doi.org/10.1016/j.ijhydene.2020.06.105.
[19] J.C.M. Silva, S. Ntais, V. Rajaraman, É. Teixeira-Neto, Â.A. Teixeira-Neto, A. O. Neto, R.M. Antoniassi, E.V. Spinacé, E.A. Baranova, The Catalytic Activity of Pt: Ru Nanoparticles for Ethylene Glycol and Ethanol Electrooxidation in a Direct Alcohol Fuel Cell, Electrocatalysis 10 (2019) 203–213, https://doi.org/10.1007/s12678-019-00515-8.
[20] J.C.M. Silva, S. Ntais, É. Teixeira-Neto, E.V. Spinacé, X. Cui, A.O. Neto, E. A. Baranova, Evaluation of carbon supported platinum–ruthenium nanoparticles for ammonia electro-oxidation: Combined fuel cell and electrochemical approach, Int. J. Hydrog. Energy 42 (2017) 193–201, https://doi.org/10.1016/j.ijhydene.2016.09.135.
[21] F. Maillard, G.Q. Lu, A. Wieckowski, U. Stimming, Ru-Decorated Pt Surfaces as Model Fuel Cell Electrocatalysts for CO Electrooxidation, J. Phys. Chem. B 109 (2005) 16230–16243, https://doi.org/10.1021/jp052277x.
[22] A. Beck, H. Frey, M. Becker, L. Artiglia, M.G. Willinger, J.A. van Bokhoven, Influence of hydrogen pressure on the structure of platinum–titania catalysts, J. Phys. Chem. C. 125 (2021) 22531–22538, https://doi.org/10.1021/acs.jpcc.1c05939.
[23] G. Caballero-Manrique, E. Brillas, F. Centellas, J.A. Garrido, R.M. Rodríguez, P.-L. Cabot, Electrochemical oxidation of the carbon support to synthesize Pt(Cu) and Pt-Ru(Cu) core-shell electrocatalysts for low-temperature fuel cells, Catalysts (2015) 815–837, https://doi.org/10.3390/catal5020815.
[24] C. Molochas, P. Tsiakaras, Carbon Monoxide Tolerant Pt-based electrocatalysts for H2-PEMFC applications: current progress and challenges, Catalysts (2021), https://doi.org/10.3390/catal11091127.
[25] E.H. Fontes, C.E.D. Ramos, J. Nandenha, R.M. Piasentin, A.O. Neto, R. Landers, Structural analysis of PdRh/C and PdSn/C and its use as electrocatalysts for ethanol oxidation in alkaline medium, Int. J. Hydrog. Energy 44 (2019) 937–951, https://doi.org/10.1016/j.ijhydene.2018.11.049.
[26] J. Li, C. Wang, X. Chen, Y. Zhang, Y. Zhang, K. Fan, L. Zong, L. Wang, Flash synthesis of ultrafine and active NiRu alloy nanoparticles on N-rich carbon nanotubes via joule heating for efficient hydrogen and oxygen evolution reaction, J. Alloy. Compd. 959 (2023) 170571, https://doi.org/10.1016/j.jallcom.2023.170571.
[27] Y. Qiu, Z. Hu, H. Li, Q. Ren, Y. Chen, S. Hu, Hybrid electrocatalyst Ag/Co/C via flash Joule heating for oxygen reduction reaction in alkaline media, Chem. Eng. J. 430 (2022) 132769, https://doi.org/10.1016/j.cej.2021.132769.
[28] R.F.B. de Souza, G.A. Silvestrin, F.G. Da Conceição, V.A. Maia, L. Otubo, A.O. Neto, E.P. Soares, Innovative lead-carbon battery utilizing electrode-electrolyte assembly inspired by PEM-FC architecture, J. Energy Storage 86 (2024) 111418, https://doi.org/10.1016/j.est.2024.111418.
[29] R.F.B. De Souza, É.T. Neto, M.L. Calegaro, E.A. Santos, H.S. Martinho, M.C. dos Santos, Ethanol Electro-oxidation on Pt/C Electrocatalysts: An "In Situ" Raman Spectroelectrochemical Study, Electrocatalysis 2 (2011) 28–34, https://doi.org/10.1007/s12678-010-0031-0.
[30] J.-D. Qiu, G.-C. Wang, R.-P. Liang, X.-H. Xia, H.-W. Yu, Controllable Deposition of Platinum Nanoparticles on Graphene As an Electrocatalyst for Direct Methanol Fuel Cells, J. Phys. Chem. C. 115 (2011) 15639–15645, https://doi.org/10.1021/jp200580u.
[31] F. Şen, G. Gökağaç, Activity of carbon-supported platinum nanoparticles toward methanol oxidation reaction: role of metal precursor and a new surfactant, tert-octanethiol, J. Phys. Chem. C. 111 (2007) 1467–1473, https://doi.org/10.1021/jp065809y.
[32] H.-F. Cui, J.-S. Ye, W.-D. Zhang, J. Wang, F.-S. Sheu, Electrocatalytic reduction of oxygen by a platinum nanoparticle/carbon nanotube composite electrode, J. Electroanal. Chem. 577 (2005) 295–302, https://doi.org/10.1016/j.jelechem.2004.12.004.
[33] A. López-Cudero, Á. Cuesta, C. Gutiérrez, Potential dependence of the saturation CO coverage of Pt electrodes: The origin of the pre-peak in CO-stripping voltammograms. Part 2: Pt(100), J. Electroanal. Chem. 586 (2006) 204–216, https://doi.org/10.1016/j.jelechem.2005.10.003.
[34] A. Cuesta, A. Couto, A. Rincón, M.C. Pérez, A. López-Cudero, C. Gutiérrez, Potential dependence of the saturation CO coverage of Pt electrodes: the origin of the pre-peak in CO-stripping voltammograms. Part 3: Pt(poly), J. Electroanal. Chem. 586 (2006) 184–195, https://doi.org/10.1016/j.jelechem.2005.10.006.
[35] G. García, M.T.M. Koper, Stripping voltammetry of carbon monoxide oxidation on stepped platinum single-crystal electrodes in alkaline solution, Phys. Chem. Chem. Phys. 10 (2008) 3802–3811, https://doi.org/10.1039/B803503M.
[36] W. Ji, W. Qi, S. Tang, H. Peng, S. Li, Hydrothermal synthesis of ultrasmall Pt nanoparticles as highly active electrocatalysts for methanol oxidation, Nanomaterials (2015) 2203–2211, https://doi.org/10.3390/nano5042203.
[37] M.J.S. Farias, W. Cheuquepan, G.A. Camara, J.M. Feliu, Disentangling catalytic activity at terrace and step sites on selectively ru-modified well-ordered pt surfaces probed by co electro-oxidation, ACS Catal. 6 (2016) 2997–3007, https://doi.org/10.1021/acscatal.6b00439.
[38] W. Luo, Y. Jiang, M. Wang, D. Lu, X. Sun, H. Zhang, Design strategies of Pt-based electrocatalysts and tolerance strategies in fuel cells: a review, RSC Adv. 13 (2023) 4803–4822, https://doi.org/10.1039/D2RA07644F.